Tunneling characteristics for Bi2212 intrinsic josephson junctions with little influence of self-heating using short pulse technique on 60 ns time scale

AUTHOR(S):

Anagawa, K; Yamada, Y; Watanabe, T; Suzuki, M

Tunneling Characteristics for Bi2212 Intrinsic Josephson Junctions With Little Influence of Self-Heating Using Short Pulse Technique on 60 ns Time Scale

Kenkichi Anagawa, Yoshiharu Yamada, Takao Watanabe, and Minoru Suzuki

***Abstract*—A small mesa structure (10 μm $\times$ 10 μm, 15 nm thick) of intrinsic Josephson junctions in $Bi_2Sr_2CaCu_2o_{8+\delta}$ is employed to observe the tunneling characteristics and the superconducting gap magnitude by short pulse technique (short pulse interlayer tunneling spectroscopy). In the measurement on 60 ns time scale, the effect of self-heating is almost negligible in the sample, whose resistivity is as small as 10 Ωcm. In slightly overdoped region, the maximum Josephson current density increases from 0.85 to 2.1 kA/cm^2 with increasing doping level. The superconducting gap magnitude 2Δ decreases from 62 to 37 meV with increasing doping level. The value for $2\Delta/k_BT_c$ decreases from 8.3 to 5.2 with increasing doping level. These values in slightly overdoped region are smaller than those in optimum and underdoped region.**

***Index Terms*—$Bi_2Sr_2CaCu_2O_{8+\delta}$, high-temperature superconductor, intrinsic Josephson junction, pseudogap, superconducting gap, tunneling spectroscopy.**

I. Introduction

THE Josephson tunneling junctions with superconductor/insulator/superconductor structure are the basic elements in the cryoelectronics based on superconductors [1]. When a high-T_c superconductor (HTSC) was found, as a matter of course, it was expected that the application of superconductivity would be expanded. However, at least as far as the Josephson devices are concerned, those with HTSC are not necessarily put to practical use so far. This is mainly because it is difficult to fabricate the Josephson tunneling junction with oxide HTSC whose performance is comparable to those with the conventional superconductor. On the other hand, it has been found that in strongly anisotropic HTSC such as $Bi_2Sr_2CaCu_2O_{8+\delta}$ (Bi2212), all CuO_2 planes are connected by the Josephson effect [2]. These built-in tunnel junctions in a layered crystal structure are called the intrinsic Josephson junctions (IJJ's). Among the various Josephson junctions with HTSC, the IJJ is found to be an ideal tunneling junction with a flat interface between superconductor and insulator in atomic scale. A large study on IJJ is now under way to put them to practical use [3].

IJJ can also be used for tunneling spectroscopy, which is a technique that directly probes the electronic states of a metal or a superconductor [4]. This technique, which is called interlayer tunneling spectroscopy (ITS), [5], [6] is free from surface problems that obscure the original properties. Moreover, it is an advantage of this technique that the probed part can be characterized by transport measurements, providing a solid basis and reliability for the specimen that yielded the results. On the other hand, self-heating, which is a problem associated with ITS, occurs when a large current is injected. Short-pulse technique on a 600 ns time scale has ever been employed and demonstrated that it is effective to reduce self-heating [7]. Owing to these advantages, short-pulse ITS has revealed, for instance, the coexistence of the superconducting gap (SG) and the pseudogap (PG) in underdoped and optimally doped Bi2212 [8]. However, it was found in overdoped samples that self-heating shows up again even on a submicrosecond time scale since their resistivity is lower than that of optimum or underdoped samples. Studies on overdoped Bi2212 are still necessary because their maximum Josephson current density is larger and suitable for the application. Therefore, it is imperative for the short pulse ITS technique to operate on shorter time scale than previously to investigate overdoped samples.

This paper reports a short pulse ITS technique on a time scale as short as 60 ns using an impedance-matched measurement system. This technique enables us to observe the SG with little influence of self-heating even in overdoped sample, and we have found that the value for $2\Delta/k_BT_c$ decreases from 8.3 to 5.2 with increasing doping level. These values in slightly overdoped region are smaller than those in optimum and underdoped region [9].

II. Experimental

A. Characterization of Samples

The samples with the mesa structure were fabricated on a cleaved surface of Bi2212 single crystal. The mesa pattern area S is ranging from 24 to 94 μm^2 and its thickness is about 15 nm. This value corresponds to $N = 10$, where N is the number of IJJ's in the mesa. The sample has a three-terminal configuration, as shown in Fig. 1(c). The top of the mesa is covered with a 425 nm thick Au upper electrode, which is effective to remove

Manuscript received October 5, 2004. This work was supported in part by the Mitsubishi Foundation.

K. Anagawa, Y. Yamada, and M. Suzuki are with the Department of Electronic Science and Engineering, Kyoto University, Kyoto 615-8510, Japan (e-mail: anagawa@sk.kuee.kyoto-u.ac.jp).

T. Watanabe is with the NTT photonics Laboratories, Kanagawa 243-0198, Japan.

Digital Object Identifier 10.1109/TASC.2005.849748

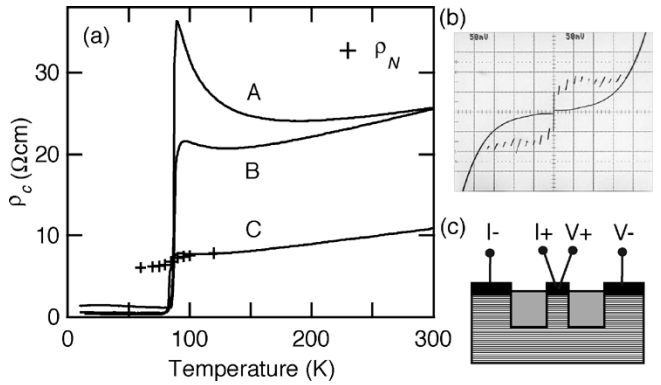

Fig. 1. (a) Temperature dependences of ρ_c for Samples A–C. $\rho_N(t = 60\,\mathrm{ns}, V = 1\,\mathrm{V})$ for Sample C is plotted at various temperatures. (b) An oscilloscope image of the I-V characteristics for Sample C measured at 11 K. X-axis: 50 mV/div, Y-axis: 0.5 mA/div. (c) A schematic of the sample.

TABLE I
VALUES FOR T_c, N, AND S OF SAMPLES A–D

Sample	A	B	C	D
T_c (K)	87	87.5	83	82
N	10	7	10	7
S (μm^2)	94	83	54	24

the heat generated in the mesa by current injection. The sample fabrication was described in detail elsewhere [10].

Fig. 1(a) shows the temperature dependences of the mesa resistivity $\rho_c(T)$ of Samples A–C in the c-axis direction. T_c for the sample is estimated from the resistive transition in Fig. 1(a). The values for T_c of Samples A–D are listed in Table I. Samples A–C are found to be slightly overdoped from the decrease of $\rho_c(T)$ with temperature near 300 K in Fig. 1(a) [6], [11]. In Sample C, the value for ρ_c is smaller than the half of that for Sample A and $\rho_c(T)$ shows rather metallic behavior than semiconductive behavior above T_c, as seen in the curve of Sample A. Thus, Sample C is a little more overdoped than the other samples. Such sample has a smaller normal tunneling resistance R_N and can be overheated by the larger self-injection current.

Fig. 1(b) shows an oscilloscope image of the current (I)-voltage (V) characteristics for Sample C measured at 11 K. The number of junctions N in this sample is 10, as seen in the number of resistive branches. The maximum Josephson current I_c was estimated to be 0.9 mA from the resistive branch in Fig. 1(b).

In the measurement using the three-terminal sample, the contact resistance R_{cont} in the upper electrode should be much smaller than the sample resistance. In Fig. 1(a), Sample B has rather large R_{cont} than that of the other samples and its value was estimated to be 1.4 Ω from the residual resistance of the sample below T_c. This value is no greater than 6% of R_c(300 K). In addition, the voltage reduction in R_{cont} is much smaller than that in normal resistance, because R_{cont} usually has nonlinearity. Therefore, R_{cont} is neglected in the data analysis.

B. Measurement System Setup

We constructed an impedance-matched measurement system to reduce voltage ripples superposed on pulses, which prevent precise measurements on a shorter than sub-μs time scale. In the measurement system, the sample was connected to an arbitrary waveform generator with an output impedance of 50 Ω and to a four-channel digital oscilloscope with an input impedance of 50 Ω via 50 Ω cryogenic coaxial cables. We used the composite current pulses of 1.2 μs width, which consist of three parts: a sharp rise part of 30 ns width, a flat part of 700 ns width, and a smooth fall part of 500 ns width like a quarter-period sinusoidal curve.

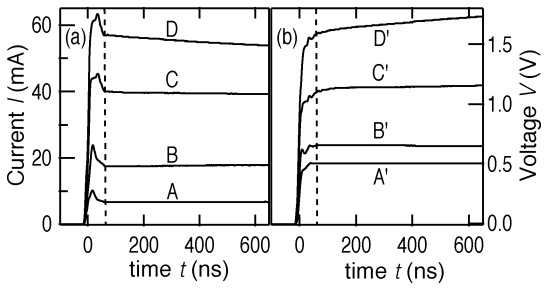

Fig. 2. (a) Current and (b) voltage pulse responses measured at 10 K for Sample A. The broken line indicates the data acquirement time of $t = 60$ ns.

III. RESULTS AND DISCUSSION

A. Influence of Self-Heating

Fig. 2 shows the current and voltage pulse responses at 4 input levels from Sample A at 10 K. In the responses, no significant ripple is seen after 60 ns from the rise of a pulse, enabling the short pulse ITS on the 60 ns time scale. We define, respectively, $I(t)$ and $V(t)$ for a pulse as the magnitude of the current and voltage as a function of time t after the rise of a pulse. The curves A and A′ in Figs. 2(a) and (b) show $I(t)$ and $V(t)$ at a level of $V(60\,\mathrm{ns}) = 0.50$ V, which is smaller than the SG voltage of $V_g = 0.65$ V. Both responses show a flat t-dependence, indicating clearly the absence of the self-heating. At this current level, I-V curves scarcely suffer from the influence of self-heating even on a 0.6 μs time scale. The curves B and B′ show the pulse responses near V_g. The t-dependence is still flat and there is little difference between $V(60\,\mathrm{ns})$ and $V(600\,\mathrm{ns})$, showing again little influence from the self-heating at this current level.

At larger voltages, however, $I(t)$ and $V(t)$ start to show an appreciable t-dependence. For Curve C for current density $J \sim 40\,\mathrm{kA/cm^2}$ and area-normalized power $Q \sim 44\,\mathrm{kW/cm^2}$, $I(600\,\mathrm{ns})$ is smaller than $I(60\,\mathrm{ns})$ by 2%. For Curve C′, $V(600\,\mathrm{ns})$ is larger than $V(60\,\mathrm{ns})$ by 5%. The conductance, $\sigma(600\,\mathrm{ns}) = I(600\,\mathrm{ns})/V(600\,\mathrm{ns})$, is smaller than $\sigma(60\,\mathrm{ns})$ by 7%. Similarly the curves D and D′ at a level of $J \sim 55\,\mathrm{kA/cm^2}$ and $Q \sim 88\,\mathrm{kW/cm^2}$ show that $\sigma(600\,\mathrm{ns})$ is smaller than $\sigma(60\,\mathrm{ns})$ by 13%. The variation in $\sigma(600\,\mathrm{ns})$ from $\sigma(60\,\mathrm{ns})$ reflects the influence of self-heating. Thus, it is seen that the self-heating becomes significant as V increases, that is, as the current injection increases at $t = 600$ ns.

Fig. 3 shows the I-V curves measured in Sample A at various t from 60 to 600 ns. Josephson current in the low voltage region was suppressed by the magnetic fields (0.5 T) in the c-axis direction. Below V_g, all the I-V curves fall onto a single curve. This means that the self-heating exerts almost no influence on

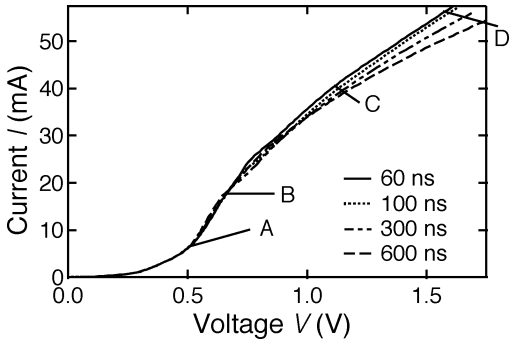

Fig. 3. I-V curves at 10 K measured at various t from 60 to 600 ns. The points indicated by A–D correspond to the current levels in Fig. 2.

the I-V curves below V_g on these time scales. For $V > V_g$, on the other hand, the I-V curve systematically deviates toward the positive V direction. Clearly, the larger the value for t, the greater is the shift in the I-V curve. This shift is caused by the self-heating since R_N increases with increasing T as shown in the inset to Fig. 3. This implies that the self-heating starts to be influential again even in the short pulse method on a 300 μs time scale.

Above T_c, the temperature rise ΔT due to self-heating can be roughly estimated from ΔR_N, an increase in R_N when V is increased, by assuming that $dR_N/dT = dR_c/dT = 21\ \mathrm{K}/\Omega$ in Sample C. At 120 K, R_N measured at $t = 60$ ns increases by $\Delta R_N \approx 1.1\ \Omega$ from $V = 1$ V up to 1.3 V, and hence $\Delta T < 25$ K. In the case in which $R_c = R_N$ is further assumed, $\Delta R_N = R_N - R_c = 0.2\ \Omega$ at $V = 1$ V in Sample C, as seen in Fig. 1(c), ΔT could be estimated to be no higher than 5 K. However, the estimate for R_N in Sample C includes an uncertainty of 0.5 Ω, which implies a ΔT uncertainty of 10 K. Consequently, in the sample with small value for ρ_c, such as Sample C, the influence of self-heating is little significant in the tunneling characteristics measured at $t = 60$ ns.

Below T_c, it is difficult to estimate ΔT from ΔR_N because of strong nonlinearity in I-V curves.

B. Tunneling Characteristics

Fig. 4(a) shows the $dI/dV - V$ characteristics measured at various $t = 60$ ns at various temperatures for Sample B. In this figure, the abscissa indicates the voltage normalized by N. The sharp conductance peak corresponds to the SG structure below T_c. The depletion in low voltage characteristics corresponds to the pseudogap (PG) structure above T_c. The flat characteristics at 140 K indicates that the PG structure disappears. This is consistent with the almost linear temperature dependence of $\rho_c(T)$ in Sample B at 140 K [6].

The gap magnitude $2\Delta_{\mathrm{SG}}$ and $2\Delta_{\mathrm{PG}}$ for SG and PG, respectively, are defined from the half of the conductance peak separation. $2\Delta_{\mathrm{SG}}$ for Sample B is estimated to be 50 meV at 10 K. $2\Delta_{\mathrm{PG}}$ for Sample B is estimated to be 67 meV at 90 K. These values are consistent with the previous results in slightly overdoped region [8].

The temperature dependence of $2\Delta_{\mathrm{SG}}$ and $2\Delta_{\mathrm{PG}}$ for Sample B is exhibited in Fig. 4(b). $2\Delta_{\mathrm{SG}}(T)$ decreases monotonically with the increase in temperature below 80 K in the measurement

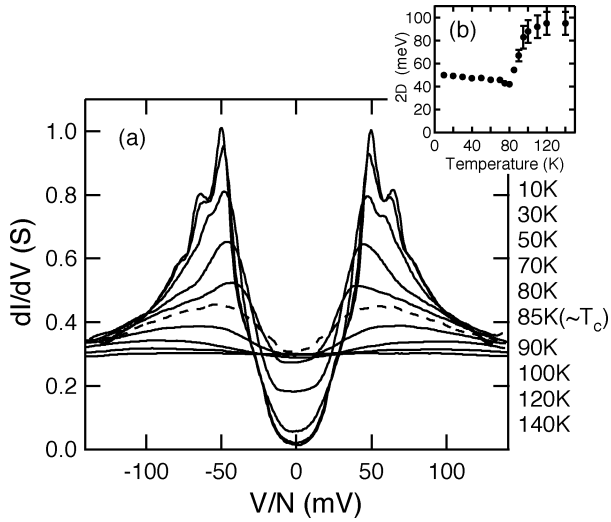

Fig. 4. (a) $dI/dV - V$ characteristics measured at $t = 60$ ns at various temperatures for Sample B. V/N is the normalized voltage for a single junction. The break line curves shows the $dI/dV - V$ characteristics at 85 K $\approx T_c$. (b) The temperature dependence of the gap magnitude 2Δ for Sample B. 2Δ is represented by $2\Delta_{\mathrm{SG}}$ below T_c and $2\Delta_{\mathrm{PG}}$ above T_c.

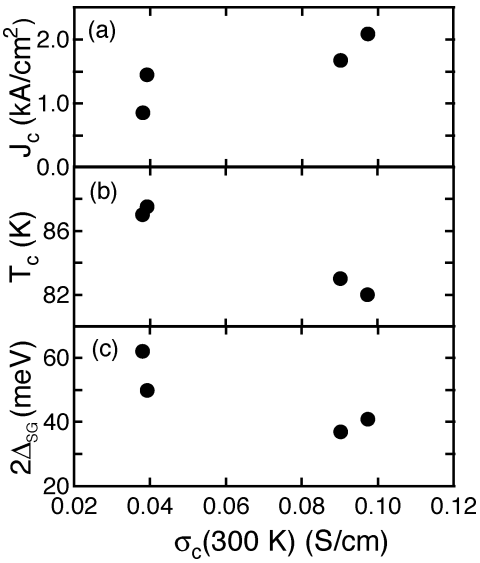

Fig. 5. The doping dependence of (a) J_c, (b) T_c, and (c) $2\Delta_{\mathrm{SG}}$. $2\Delta_{\mathrm{SG}}$ is represented by the value for $2\Delta_{\mathrm{SG}}(T)$ at 10 K. $\sigma_c(300\ \mathrm{K})$ is the reference of the doping level in the samples.

on 60 ns time scale with little influence of self-heating. This indicates that the SG closes at T_c in HTSC. $2\Delta_{\mathrm{PG}}(T)$ increases with increasing temperature and remains almost unchanged above 100 K. The behavior of both $2\Delta_{\mathrm{SG}}(T)$ and $2\Delta_{\mathrm{PG}}(T)$ agrees with the previous results [6].

C. Doping Dependence

Figs. 5(a)–(c) show the doping dependence of the maximum Josephson current density J_c, T_c, and, $2\Delta_{\mathrm{SG}}(10\ \mathrm{K})$, respectively. The value for the conductivity at 300 K of the samples, $\sigma_c(300\ \mathrm{K})$ is the reference of the doping level in the samples. In Fig. 5(a), J_c increases from 0.85 to 2.1 $\mathrm{kA/cm^2}$ with increasing doping level. This is consistent with the doping dependence of J_c in IJJ's of Bi2212 [12] and $Bi_2Sr_2Ca_2Cu_3O_{10+\delta}$ [13].

Figs. 5(b) and (c) show that both T_c and $2\Delta_{\mathrm{SG}}(10\ \mathrm{K})$ have a tendency to decrease with increasing doping level in slightly overdoped region. T_c decreases from 87.5 to 82 K and $2\Delta_{\mathrm{SG}}(10\ \mathrm{K})$ decreases from 62 to 37 meV. In Sample D, T_c is smaller than that in Sample A by $\sim$6% and $2\Delta_{\mathrm{SG}}(10\ \mathrm{K})$ is smaller than that in Sample A by $\sim$34%. Thus, it is found that the value for $2\Delta_{\mathrm{SG}}/\mathrm{k}_B T_c$ decreases from 8.3 to 5.2 with increasing doping level in slightly overdoped region. These values are smaller than those in optimum and underdoped region [9].

REFERENCES

[1] A. Barone and G. Paternò, *Physics and Applications of the Josephson Effect*: Wiley, 1982.

[2] R. Kleiner and P. Müller, "Intrinsic Josephson effects in high-T_c superconductors," *Phys. Rev. B*, vol. 49, pp. 1327–1341, Jan. 1994.

[3] A. A. Yurgens, "Intrinsic Josephson junctions: recent developments," *Supercond. Sci. Technol.*, vol. 13, pp. R85–R100, Aug. 2000.

[4] I. Giaever, "Energy gap in superconductors measured by electron tunneling," *Phys. Rev. Lett.*, vol. 5, pp. 147–148, Aug. 1960.

[5] M. Suzuki, S. Karimoto, and K. Namekawa, "Interlayer tunneling spectroscopy and evidence of a pseudogap in $\mathrm{Bi_2Sr_2CaCu_2O_8}$," *J. Phys. Soc. Jpn.*, vol. 67, pp. 732–735, Mar. 1998.

[6] M. Suzuki, T. Watanabe, and A. Matsuda, "Interlayer tunneling spectroscopy for slightly overdoped $\mathrm{Bi_2Sr_2CaCu_2O_{8+\delta}}$," *Phys. Rev. Lett.*, vol. 82, pp. 5361–5364, June 1999.

[7] ——, "Short pulse tunneling measurements of the intrinsic Josephson junctions in Bi-Sr-Ca-Cu-O," *IEEE Trans. Appl. Supercond.*, vol. 9, pp. 4507–4510, Jun. 1999.

[8] M. Suzuki and T. Watanabe, "Discriminating the superconducting gap from the pseudogap in $\mathrm{Bi_2Sr_2CaCu_2O_{8+\delta}}$ by interlayer tunneling spectroscopy," *Phys. Rev. Lett.*, vol. 85, pp. 4787–4790, Nov. 2000.

[9] A. Matsuda, S. Sugita, and T. Watanabe, "Temperature and doping dependence of the $\mathrm{Bi_2Sr_{1.9}CaCu_2O_{8+\delta}}$ pseudogap and superconducting gap," *Phys. Rev. B*, vol. 60, pp. 1377–1381, Jul. 1999.

[10] K. Tanabe, Y. Hidaka, S. Karimoto, and M. Suzuki, "Observation of both pair and quasiparticle tunneling in intrinsic junction stacks fabricated on $\mathrm{Bi_2Sr_2CaCu_2O_{8+\delta}}$ single crystals," *Phys. Rev. B*, vol. 53, pp. 9348–9352, Apr. 1996.

[11] T. Watanabe, T. Fujii, and A. Matsuda, "Anisotropic resistivities of precisely oxygen controlled single-crystal $\mathrm{Bi_2Sr_2CaCu_2O_{8+\delta}}$: systematic study on "Spin Gap" effect," *Phys. Rev. Lett.*, vol. 79, pp. 2113–2116, Sep. 1997.

[12] K. Inomata, T. Kawae, K. Nakajima, S.-J. Kim, and T. Yamashita, "Junction parameter control of $\mathrm{Bi_2Sr_2CaCu_2O_{8+\delta}}$ stacked junctions by annealing," *Appl. Phys. Lett.*, vol. 82, pp. 769–771, Feb. 2003.

[13] Y. Yamada, K. Anagawa, T. Shibauchi, T. Fujii, T. Watanabe, A. Matsuda, and M. Suzuki, "Interlayer tunneling spectroscopy and doping-dependent energy-gap structure of the trilayer superconductor $\mathrm{Bi_2Sr_2Ca_2Cu_3O_{10+\delta}}$," *Phys. Rev. B*, vol. 68, pp. 054 533-1–054 533-11, Aug. 2003.